JOURNAL OF MATERIALS SCIENCE 30 (1995) 5819–5824

Influence of temperature on the low- and high-frequency relaxation in a TTB-type ferroelectric relaxor $Pb_2K(Nb_{0.1}Ta_{0.9})_5O_{15}$

Z. LU*, J.-P. BONNET‡, J. RAVEZ, P. HAGENMULLER
Laboratoire de Chimie du Solide du CNRS, Université de Bordeaux I, 351, cours de la Libération, 33405 Talence Cedex, France

Dielectric measurements on $Pb_2K(Nb_{0.1}Ta_{0.9})_5O_{15}$ ceramics have been reported at $140 < T < 530$ K in the 20–10^9 Hz frequency range. The tetragonal tungsten bronze-type (TTB) material shows a typical ferroelectric relaxor behaviour. Three dielectric dispersions are observed. The relaxor behaviour results from a thermally activated relaxation with a large time distribution. This relaxation could be interpreted in terms of a polar microdomain concept. The two other dielectric dispersions result from a space charge effect and from a relaxation probably related to the TTB structure.

1. Introduction

Relaxor behaviour has already been reported for ferroelectrics showing a diffuse phase transition (DPT) [1–5]. DPT may occur when different cations occupy equivalent sites of the crystal lattice. The high relative permittivity and broad $\varepsilon'_r = f(T)$ peak observed for such materials are promising properties for applications such as multilayer capacitors. One of the most interesting ferroelectric relaxors is $Pb(Mg_{1/3}Nb_{2/3})O_3$, which exhibits very high dielectric constant ($\varepsilon'_r > 10^4$) and low dielectric losses ($\tan\delta < 10^{-2}$) at room temperature [6]. Its Curie temperature is about 265 K and the phase transition occurs in a temperature range of several tens of degrees.

Most research concerning ferroelectric relaxors has concentrated on perovskite-type materials. However, a relaxor behaviour has been recently observed for $Cd_2Nb_2O_7$, a ferroelectric ceramic with pyrochlore structure [7], and for tetragonal tungsten bronze-type (TTB) ferroelectrics [8, 9].

Even though the study of the relaxation processes may lead to information concerning the origin of the DPT behaviour and high dielectric constant, only a few works [9, 10] have been devoted to the investigation of dielectric relaxations in ferroelectric relaxor.

This paper presents results concerning the influence of temperature and frequency on the dielectric properties of a TTB-type ferroelectric ceramic of composition $Pb_2K(Nb_{0.1}Ta_{0.9})_5O_{15}$ ($PKN_{0.1}T_{0.9}$) material which presents a diffuse phase transition [11] and a relaxor behaviour.

2. Experimental procedure

2.1. Ceramic preparation

The powdered $PKN_{0.1}T_{0.9}$ was prepared according to the following chemical reaction

$$4PbO + K_2CO_3 + 0.5Nb_2O_5 + 4.5Ta_2O_5 \rightarrow 2Pb_2K(Nb_{0.1}Ta_{0.9})_5O_{15} + CO_2 \quad (1)$$

The starting constituents (PbO, 99.9% Aldrich; K_2CO_3, > 99.0% Merck; Nb_2O_5, 99.9% Aldrich; Ta_2O_5, 99.9% Prolabo) were mixed in an agate grinder for 1 h in pure ethanol. The mixture was then put into an alumina vessel and calcined at 1100 °C for 15 h. The obtained material was examined by X-ray diffraction (XRD) with silicon as internal standard.

The method used for the preparation of $PKN_{0.1}T_{0.9}$ ceramic was the same as that reported previously for $Pb_2KNb_5O_{15}$ [12]. To prevent a PbO volatilization, the sintering of $PKN_{0.1}T_{0.9}$ + 0.5 wt % PbO pellets (diameter 10 mm, thickness ~ 1.6 mm) was carried out at 1460 °C, for 1 h, in a closed alumina vessel.

2.2 Dielectric measurements

The sample preparation and the detailed experimental procedure used for low-frequency measurements have been described elsewhere [12]. Permittivity was recorded over the temperature range 140–530 K with a computer-controlled impedance analyser (Wayne-Kerr 6425 A) at selected frequencies between 20 and 3×10^5 Hz.

For high-frequency measurements, diameter and thickness of the samples were reduced to 6.95 ± 0.05 mm and about 1 mm, respectively. Gold was sputtered on a circular surface of 3 mm diameter at the centre of one face, while the other face and the edge of the sample were completely covered with gold. The measurements were performed from 230–330 K in the 10^6–10^9 Hz frequency range using a coaxial method [13] and a HP8753 A network analyser. The real, ε'_r, and imaginary, ε''_r, parts of the permittivity

* *Present address*: Laboratoire de Chimie-Physique du Solide, Ecole Centrale de Paris, 92295 Châtenay-Malabry Cedex, France.
‡ *Present address*: ENSCI, 47, Avenue Albert Thomas, 87065 Limoges Cedex, France.

0022–2461

were calculated from the complex admittance data [14].

The difference between the permittivity values determined from low- and high-frequency equipments was estimated to be less than 10%.

3. Results

3.1. Ceramic characterization

The XRD pattern of the powder obtained revealed that $PKN_{0.1}T_{0.9}$ crystallized, at room temperature, with a tetragonal symmetry and a TTB-type structure ($a = 1.780 \pm 0.001$ nm, $c = 0.3935 \pm 0.0005$ nm). No parasite phases were detected.

The weight of the as-sintered ceramic was found to be 0.4 wt % lower than that corresponding to a stoichiometric compound. The ceramic relative density, determined by the Archimede's method, was about 95% theoretical (7.51 g cm^{-3}). The microstructure was observed on thermally etched samples (1400 °C, 15 min) using SEM (Jeol 840A). The average grain size was about 2 μm.

3.2. Temperature and frequency dependence of the permittivity

3.2.1. Low-frequency measurements

The evolution of the real part of the permittivity, ε'_r, versus temperature is shown in Fig. 1a for several frequencies. As expected, a maximum of ε'_r, related to the paraelectric–ferroelectric transition, is observed.

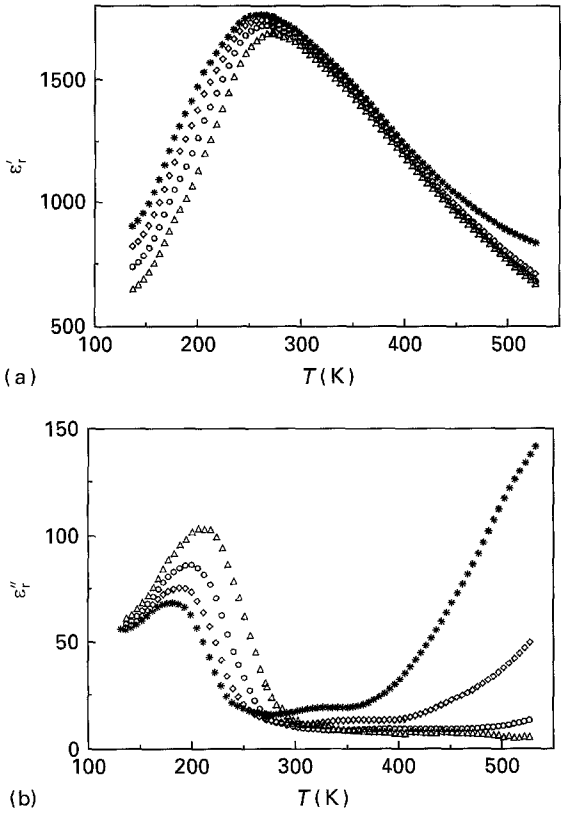

Figure 1 Temperature dependence of (a) the real, ε'_r, and (b) imaginary, ε''_r, parts of the permittivity for various frequencies ($Pb_2K(Nb_{0.1}Ta_{0.9})_5O_{15}$ ceramics): (*) 100 Hz, (◇) 1 kHz, (○) 10 kHz, (△) 100 kHz.

The peak temperature, T_m, increases with increasing frequency. This behaviour was already described as characteristic of a diffuse phase transition (DPT) [11].

The influence of the frequency on the $\varepsilon'_r = f(T)$ curve (Fig. 1a) reveals a dispersion in the ferroelectric state, whereas no appreciable dispersion is observed in the paraelectric state between 300 and 400 K. Such a behaviour is typical for a ferroelectric relaxor [2]. The absence (or weakening) of the dispersion in the paraelectric state suggests that the relaxation tends to disappear with the spontaneous polarization or/and that the dielectric relaxation in a thermally-activated process shifted towards higher frequency in the paraelectric state.

At $T > 400$ K, another dispersion is observed which weakens quickly with increasing frequency. This phenomenon appears at high temperature and low frequency when the charge carriers are sufficiently mobile; therefore, it should be linked to space charge effect. This interpretation is in agreement with the strong frequency dependence of the corresponding imaginary part of the permittivity (Fig. 1b); ε''_r is directly related to the electrical conductivity.

Comparison of Fig. 1a and b leads to the following observations:

(i) at a given frequency, the temperature of the ε''_r peak is significantly lower than that of the ε'_r peak;

(ii) at temperature lower than 250 K, one observes an opposite evolution of ε'_r and ε''_r with frequency; at rising frequency ε'_r decreases while ε''_r increases.

Both types of behaviour are usually observed for ferroelectric relaxor materials.

Dielectric dispersion can be more clearly detected by plotting ε'_r and ε''_r versus $\log_{10} f$ (Fig. 2). In the $20–3 \times 10^5$ Hz frequency range, two dispersions exist. The first one, which exists at low frequencies ($f < 10^3$ Hz) and high temperatures ($T > 400$ K), could be associated with a space charge effect. The second dispersion appears in the temperature range ($T < 274$ K) where a continuous increase of ε''_r with increasing frequency is observed.

3.2.2. High-frequency measurements

The microwave data show a peak of ε''_r at about 5×10^8 Hz, accompanied by a strong decrease of ε'_r (Fig. 3). The $\varepsilon'_r = f(\log_{10} f)$ curve corresponding to $T = 239$ K is representative of the evolution observed at $T < 274$ K. It indicates the presence of two dispersion processes in that temperature range. The existence of these two relaxations is more clearly apparent in a Cole–Cole representation (see Fig. 5b below). For simplicity, the relaxation corresponding to the strong dispersion region will be called the principal relaxation and the relaxation exhibiting a shallow dispersion will be quoted as the diffuse relaxation. The ε''_r peak frequency, f_{r2}, characterizing the principal relaxation (defined as the relaxation frequency) seems to be almost temperature independent. The relaxation frequency, f_{r1}, of the diffuse relaxation cannot be directly determined from Fig. 3.

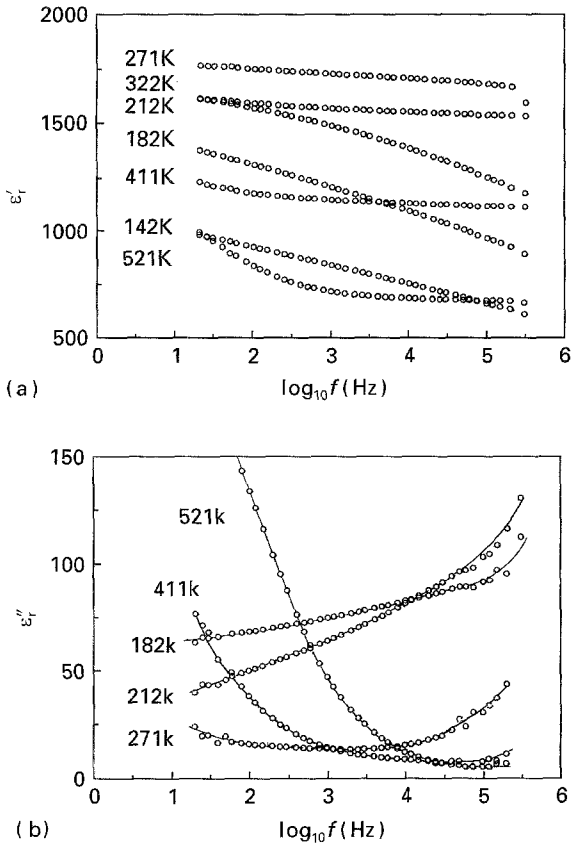

Figure 2 Influence, at various temperatures, of the frequency ($20 \leqslant f \leqslant 3\ 10^5$ Hz) on (a) the real and (b) imaginary parts of the permittivity ($Pb_2K(Nb_{0.1}Ta_{0.9})_5O_{15}$ ceramics).

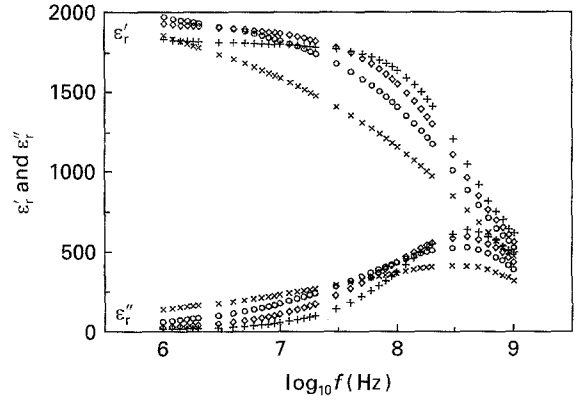

Figure 3 High-frequency ($10^6 \leqslant f \leqslant 10^9$ Hz) dielectric spectrum of $Pb_2K(Nb_{0.1}Ta_{0.9})_5O_{15}$ ceramics at various temperatures: (+) 330 K, (◇) 299 K, (○) 274 K, (×) 239 K.

4. Discussion

4.1. Space charge dispersion

The space charge dispersion does not correspond necessarily to a loss peak if it concerns a genuine bulk effect [15]. According to Jonscher [16], its contribution to the complex permittivity, ε^*_{SC}, can be expressed as

$$\varepsilon^*_{SC} = a(i\omega)^{n-1} \quad (2)$$

where a is a parameter which increases with temperature and n is an exponent ($0 < n < 1$). Therefore, the contribution of the space charge to the imaginary part of the permittivity, ε''_r, becomes stronger and even predominant over the intrinsic dielectric losses. This suggests that plots of $\log_{10} \varepsilon''_r = f(\log_{10} f)$ could lead to a straight line with a slope equal to $n - 1$ at high temperature and low frequency. Such a prevailing space charge contribution is observed at 521 K for $f \leqslant 10^3$ Hz; the value of the exponent, n, being about 0.45. A detailed quantitative treatment of the space-charge-induced dispersion has been given for $Pb_2KNb_5O_{15}$ elsewhere [12].

4.2. Diffuse and principal relaxations

Dielectric relaxation is commonly analysed using the Cole–Cole formalism [7, 10, 17]

$$\varepsilon^*_r = \frac{\Delta\varepsilon'_r}{1 + (i\omega\tau)^{1-\alpha}} + \varepsilon'_\infty \quad (3)$$

where $\varepsilon^*_r = \varepsilon'_r - i\varepsilon''_r$ is the complex permittivity. $\Delta\varepsilon'_r = \varepsilon'_s - \varepsilon'_\infty$ represents the difference between the static, ε'_s, and the high-frequency, ε'_∞, relative permittivity. τ stands for the average time constant. α is an empirical exponent taking $0 \leqslant \alpha \leqslant 1$ values and closely related to the degree of inhomogeneity of the materials. It is generally accepted that α is representative of the width of relaxation time distribution [17, 18].

The dispersion process observed at low temperature below 3.10^5 Hz (Fig. 2a and b) is the onset of the diffuse relaxation observed on the high-frequency spectra (Fig. 3). At $f \ll f_r$ ($\simeq 10^7$ Hz), equation 3 can be simplified to

$$\varepsilon^*_r = \varepsilon'_r[1 - (i\omega\tau)^{1-\alpha}] + \varepsilon'_\infty \quad (4)$$

Therefore

$$\varepsilon''_r = \Delta\varepsilon'_r(\omega\tau)^{1-\alpha}\cos(\alpha\pi/2) \quad (5)$$

which can be rewritten as

$$\varepsilon''_r = bf^{1-\alpha} = be^{(1-\alpha)\ln f} \quad (6)$$

with $b = \Delta\varepsilon'_r(2\pi\tau)^{1-\alpha}\cos(\alpha\pi/2)$

At low frequency, for a large distribution width (α close to unity), $(1 - \alpha)\ln f$ is small enough to obtain

$$\varepsilon''_r \simeq 2.3b(1 - \alpha)\log_{10} f \quad (7)$$

The quasi-linear evolution of ε''_r versus $\log_{10} f$ observed at 182 and 212 K for $f \leqslant 10^4$ Hz (Fig. 2b) is in complete agreement with Equation 7.

The existence of two relaxation processes in the 10^6–10^9 Hz frequency range suggests the equivalent circuit depicted in Fig. 4. The meaning of each electrical element is as follows.

$C_\infty = \varepsilon_0\varepsilon'_\infty S/L$ is the capacitance obtained after the relaxations. ε_0 stands for the free space permittivity. S and L are, respectively, the surface area and the thickness of the disc sample.

$C_{i0} = \varepsilon_0\varepsilon'_{i0}S/L$ is the static capacitance due to the principal relaxation ($i = 1$) or to the diffuse relaxation ($i = 2$).

$C^*_i = A_i(i\omega)^{n_i - 1}$ represents the "universal capacitance" proposed by Jonscher which can be considered,

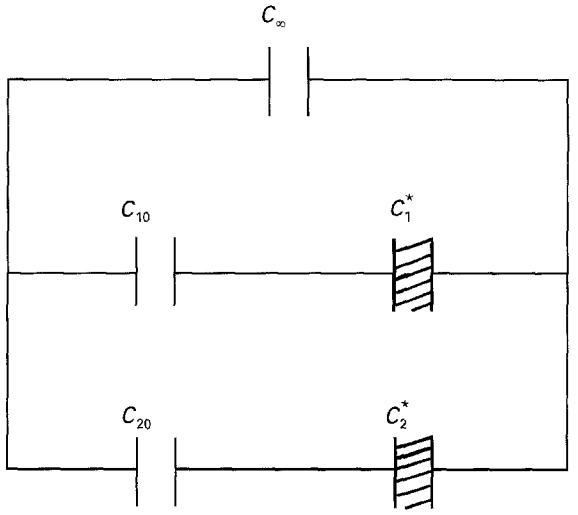

Figure 4 Equivalent circuit.

here, as a dispersive element. $A_i = a_i S/L$ is a temperature dependent parameter related to the corresponding relaxation mechanism.

A simple computation with the conventional complex method leads to the following dielectric expression

$$\varepsilon_r^* = \frac{\varepsilon'_{10}}{1 + (if/f_{r1})^{1-\alpha_1}} + \frac{\varepsilon'_{20}}{1 + (if/f_{r2})^{1-\alpha_2}} + \varepsilon'_\infty \quad (8)$$

with

$$f_{ri} = 1/2\pi(\varepsilon'_{i0}a_i)^{-1/n} \quad (9)$$

where f_{ri} and $\alpha_i = 1 - n_i$ are, respectively, the characteristic frequency and the exponent characterizing the time distribution of the ith relaxation. Equation 8 appears, in fact, as the sum of two Cole–Cole expressions (Equation 3).

Some fittings between the experimental results and the permittivities calculated from Equation 8 are illustrated in Fig. 5 for temperatures below 300 K. An excellent agreement is obtained. The value of the adjustable parameters ε'_{10}, ε'_{20}, ε'_∞, α_1, α_2, f_{r1} and f_{r2} leading to the best fit are given in Table I.

At $T > 300$ K the material is in the paraelectric state. It becomes impossible to point out whether the diffuse relaxation disappears or if merges with the principal relaxation. However, the results can be fitted quite well with a single Cole–Cole expression. This result is in agreement with the dielectric relaxation behaviour of the $Pb_2K(Nb_{1-x}Ta_x)_5O_{15}$ system ($0 \leqslant x \leqslant 1$), which supported that the diffuse relaxation disappears when the materials are completely in the paraelectric state [19].

Fig. 6 gives the temperature dependence of f_{r2} using an Arrhenius plot. f_{r2}, which increases quickly with rising temperature, is thermally activated with an activation energy of 0.20 eV. This value is comparable to those reported by Swartz *et al.* (0.17 eV) [7] and by Guo (0.24 eV) [20]. The prefactor, extrapolated at $1/T = 0$, is here 6.5×10^{11} Hz which drops in the vibration frequency range associated to ionic effects [7]. Therefore, the diffuse relaxation may be attributed to the polar domains existing in DPT materials.

The exponent α_2 decreases with increasing temperature as clearly shown in Fig. 7. Such a behaviour

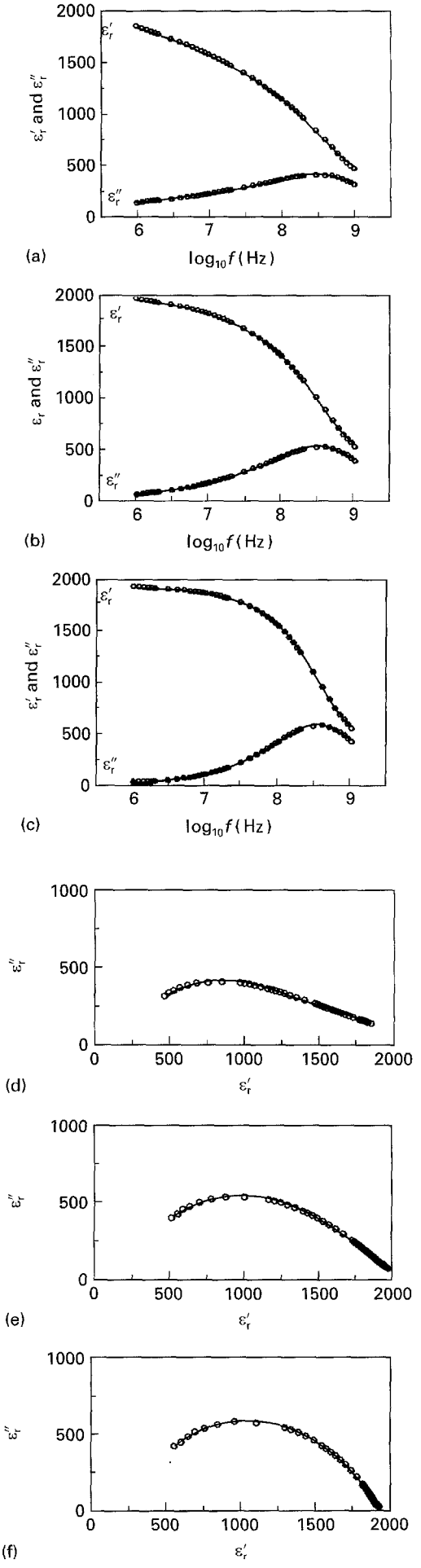

Figure 5 Comparison between the (○) experimental and (----) calculated permittivities: (a–c) ε'_r-$\log_{10} f$ and ε''_r-$\log_{10} f$ representations, and (d–f) Cole–Cole plots. (a, d) 240 K, (b, e) 274 K, (c, f) 299 K.

TABLE I Best-fit parameters for various temperatures

T(K)	f_{r2} (MHz)	f_{r1} (MHz)	α_2	α_1	ε'_{20}	ε'_{10}	ε'_{∞}
239	28.8	356	0.61	0.18	1287	686	110
246	35.9	350	0.58	0.17	1224	727	128
257	54.2	352	0.55	0.16	1101	810	148
265	76.9	353	0.51	0.14	1051	811	173
274	101	355	0.46	0.09	980	776	226
285	132	391	0.38	0.08	922	792	250
299	192	397	0.32	0.07	836	818	271

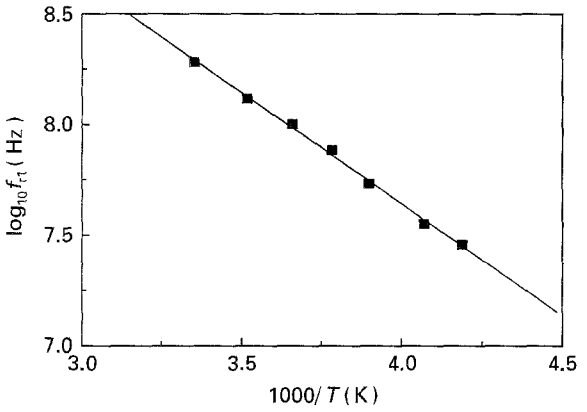

Figure 6 Arrhenius plot of the characteristic frequency of the diffuse relaxation f_{r2}.

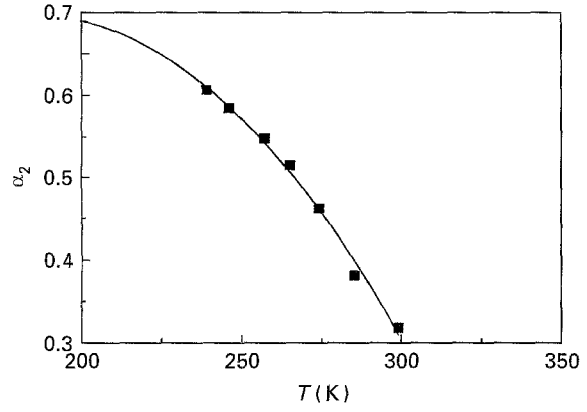

Figure 7 Influence of temperature on the factor α_2 characteristic of the relaxation time distribution of the diffuse relaxation.

implies a narrowing of the relaxation time distribution. This influence of temperature on α_2 can be easily explained by the existence of polar domains with different Curie temperature. When T is much lower than T_m the number of microdomains in the ferroelectric state is large. This situation should correspond to a large distribution of relaxation times and to a high α_2-value. As the temperature is rising, the polar domains with $T_C < T$ become non-polar and the number of remaining polar domains with different T_C is thus reduced, leading to a smaller relaxation time distribution, i.e. α_2 becomes smaller. A characteristic temperature, T_0, exists above which all the domains are non-polar; the material there is completely in the paraelectric state, the α_2 value tends to zero and the relaxation disappears. An extrapolation to $\alpha_2 = 0$ of the $\alpha_2 = f(T)$ curve (Fig. 7) yields $T_0 = 330$ K while $T_m = 265$ K.

The principal relaxation frequency, f_{r1}, however, is practically temperature independent (Table I). A similar relaxation has been already observed for some other TTB-type materials, independently of composition, preparation and processing conditions [20–23].

5. Conclusion

TTB-type ferroelectric ceramics $Pb_2K(Nb_{0.1}Ta_{0.9})_5O_{15}$ show a diffuse phase transition and a dielectric relaxor behaviour. Three dielectric dispersions have been found from 20 up to 1 GHz. The first dispersion arises from a space charge effect, which appears only at high temperatures and low frequencies. The two other dispersions are concerned with relaxation processes, which can be analysed using the Cole–Cole formalism. The relaxor behaviour results from a thermally activated relaxation ($E_a \simeq 0.20$ eV) with a large time distribution which decreases as the material tends to the paraelectric state. This relaxation, which disappears, in turn, as the material becomes paraelectric, can be interpreted using a polar microdomain concept. The principal relaxation process, not sensitive to temperature changes, exists in both ferroelectric and paraelectric states.

References

1. G. A. SMOLENSKII, *J. Phys. Soc. Jpn* **28** (suppl.) (1970) 26.
2. L.E. CROSS, *Ferroelectrics* **76** (1987) 241.
3. YAO XI, CHEN ZHILI and L. E. CROSS, *J. Appl. Phys.* **54** (1983) 3399.
4. S. J. BUTCHER and N. W. THOMAS, *J. Phys. Chem. Solids* **52** (1991) 595.
5. N. W. THOMAS, *J. Phys. Chem. Solids* **51** (1990) 1419.
6. N de MATHAN, E. HUSSON, P. GAUCHER and A. MORELL, *Mater. Res. Bull.* **25** (1990) 427.
7. S. L. SWARTZ, C. A. RANDALL and A. S. BHALLA, *J. Am. Ceram. Soc.* **72** (1989) 637.
8. T. TSURUMI and Y. HOSHINO, *ibid.* **72** (1989) 278.
9. R. GUO, A. S. BHALLA, C. A. RANDALL and L. E. CROSS, *J. Appl. Phys.* **67** (1990) 6405.
10. V. V. KIRILLOV and V. A. ISUPOV, *Ferroelectrics* **5** (1973) 3.
11. Z. G. LU, J. P. BONNET, J. RAVEZ and P. HAGENMULLER, *J. Eur. Solid State Inorg. Chem.* **30** (1993) 8.
12. LU ZHIGAO, J. P. BONNET, J. RAVEZ, J. M. RÉAU and P. HAGENMULLER, *J. Phys. Chem. Solids* **53** (1992) 1.
13. N.BELHADZ-TAHAR and A. FOURRIER-LAMER, *IEEE Trans. Microwave Theor. Tech.* **MTT 34** (1986) 346.
14. A. LARGETEAU and D. AVILES-CASTRO, *Mater. Res. Bull.* **25** (1990) 75.
15. A. K. JONSCHER, *Electrochim. Acta* **35** (1990) 1595.

16. *Idem*, "Dielectric relaxation in solids" (Chelsea Press, London, 1983).
17. K. S. COLE and R. S. COLE, *J. Chem. Phys.* **9** (1941) 341.
18. H. FRÖHLICH, "Theory of dielectric, dielectric constant and loss", 2nd Edn. (Oxford University Press, London, 1958).
19. LU ZHIGAO, Thèse 698, Université Bordeaux I (1991).
20. R. GUO, PhD Thesis, Pennsylvania State University (1990).
21. J. K. VIJI and A. M. VARAPRASAD, *Ferroelectrics* **38** (1981) 865.
22. A. M. VARAPRASAD, *Jpn J. Appl. Phys.* **24** (suppl.) (1985) 361.
23. W. L. ZHONG, P. L. ZHANG, H. C. CHEN, F. S. CHEN and Y. Y. SONG, *Ferroelectrics* **74** (1987) 325.

Received 4 January 1994
and accepted 7 June 1995